ETH zürich

Experimental Repetitive Quantum Error Correction

Gustaf Müller & Nudžeim Selimović

Supervised by: Dr. Anton Potočnik

Overview

Introduction

- Goal: protect quantum information from errors due to decoherence and other quantum noise.
- Essential to achieve fault-tolerant quantum computation.
- Deal with noise on stored quantum information, faulty quantum gates, faulty quantum preparation, and faulty measurements.

Key idea:

- ***encode*** the message - add redundant information to the message
- ***redundancy*** protects the message against the noise
- ***decode*** the message so that original message is recovered

Classical example

- Binary symmetric channel:

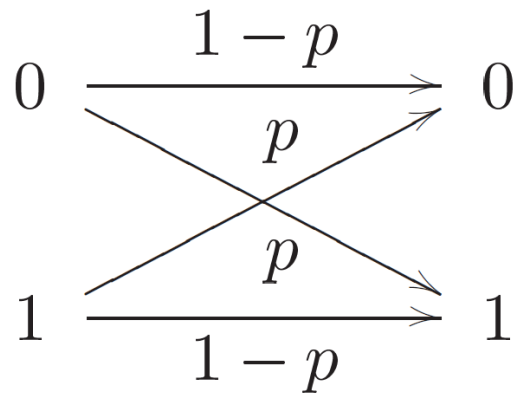

Figure: Binary symmetric channel.

- Encoding: repetition code $\Rightarrow$ 0 $\rightarrow$ 000 and 1 $\rightarrow$ 111.
- Decoding: majority voting.
- New error probability: $p_e = 3p^2 - 2p^3 \Rightarrow$ more reliable when $p < 1/2$.

Quantum error-correcting codes

Difficulties:

- ***No cloning***: duplicating the quantum states is forbidden.
- ***Errors are continuous***: appears that we need infinite precision.
- ***Measurements destroy quantum information*** observations would make recovery impossible.

Example: Bit flip channel, $a|0\rangle + b|1\rangle \longrightarrow a|1\rangle + b|0\rangle$
Probability p: $|\psi\rangle \longrightarrow X|\psi\rangle$.

Encoding:

$$|\psi\rangle = a|0\rangle + b|1\rangle$$
$$|0\rangle \longrightarrow |0_L\rangle \equiv |000\rangle$$
$$|1\rangle \longrightarrow |1_L\rangle \equiv |111\rangle$$
$$a|000\rangle + b|111\rangle$$

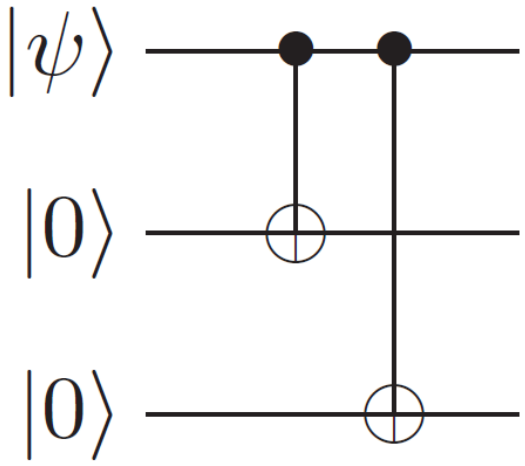

Figure: Bit flip code encoding.

Error correction procedure

- ***Error-detection***: error syndromes correspond to four projection operators:

$$P_0 \equiv |000\rangle\langle 000| + |111\rangle\langle 111| \,\text{no error}$$
$$P_1 \equiv |100\rangle\langle 100| + |011\rangle\langle 011| \,\text{bit flip on qubit 1}$$
$$P_2 \equiv |010\rangle\langle 010| + |101\rangle\langle 101| \,\text{bit flip on qubit 2}$$
$$P_1 \equiv |001\rangle\langle 001| + |110\rangle\langle 110| \,\text{bit flip on qubit 3}$$

  $\langle\psi| P_2 |\psi\rangle = 1 \;\Rightarrow\; \text{bit flip on qubit 2}$
  Syndrome measurement *does not change the state* $a|010\rangle + b|101\rangle$
  We *cannot infer anything* about the values of a and b.

- ***Recovery***: error syndrome tells us what procedure to use to recover the initial state.
- Probability for an error: $3p^2 - 2p^3$, improvement for $p < 1/2$.

Phase flip code

Probability p: $a|0\rangle + b|1\rangle \longrightarrow a|0\rangle - b|1\rangle$.
Idea: switch to basis $|+\rangle = \left(a|0\rangle + b|1\rangle\right)/\sqrt{2}$, $|-\rangle = \left(a|0\rangle - b|1\rangle\right)/\sqrt{2}$.
Operator Z acts like a bit flip, it takes $|+\rangle$ to $|-\rangle$.

Encoding:

$$|\psi\rangle = a|0\rangle + b|1\rangle$$

$$|0\rangle \longrightarrow |0_L\rangle \equiv |+++\rangle$$

$$|1\rangle \longrightarrow |1_L\rangle \equiv |---\rangle$$

$$a|+++\rangle + b|---\rangle$$

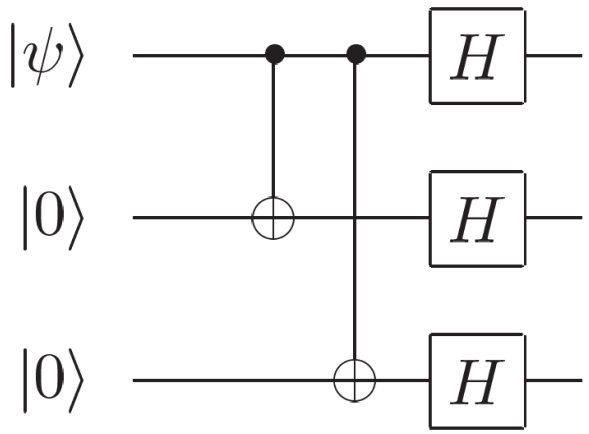

Figure: Phase flip code encoding.

Experimental Repetitive Quantum Error Correction

Philipp Schindler,[1] Julio T. Barreiro,[1] Thomas Monz,[1] Volckmar Nebendahl,[2] Daniel Nigg,[1] Michael Chwalla,[1,3] Markus Hennrich,[1*] Rainer Blatt[1,3]

The computational potential of a quantum processor can only be unleashed if errors during a quantum computation can be controlled and corrected for. Quantum error correction works if imperfections of quantum gate operations and measurements are below a certain threshold and corrections can be applied repeatedly. We implement multiple quantum error correction cycles for phase-flip errors on qubits encoded with trapped ions. Errors are corrected by a quantum-feedback algorithm using high-fidelity gate operations and a reset technique for the auxiliary qubits. Up to three consecutive correction cycles are realized, and the behavior of the algorithm for different noise environments is analyzed.

- The first experimental implementation with multiple quantum error corrections (QEC) cycles.
- Measurement- free QEC algorithm.
- $^{40}Ca^{+}$ ions as qubits.

Each QEC cycle consists of:

- encoding the system qubit $\{|0\rangle, |1\rangle\}$ and two auxiliary qubits (ancillas) into an entangled state,
- error incidence,
- detecting and correcting the error,
- resetting the ancillas.

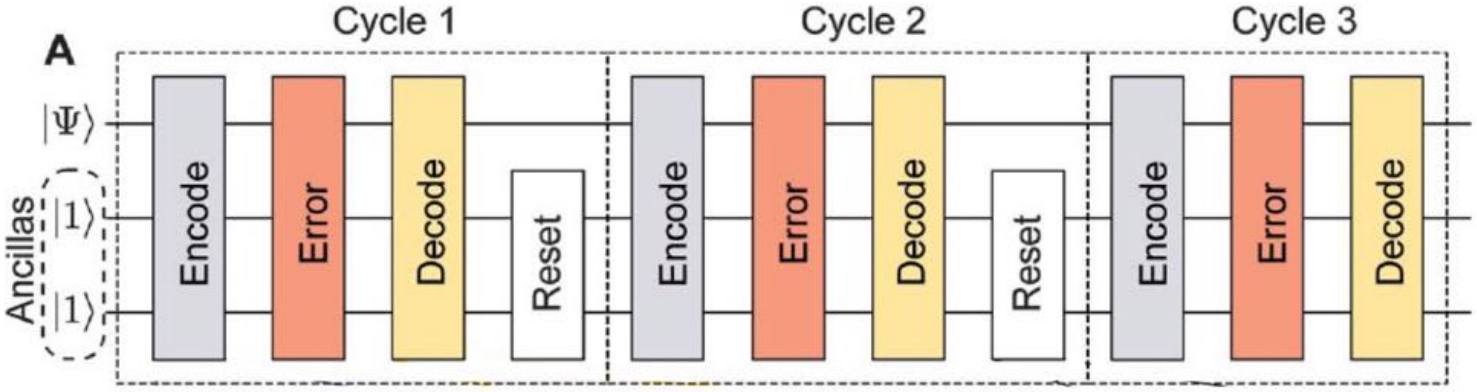

Figure: Schematic view of QEC cycles.

- Initially: $|\psi\rangle = \alpha\,|+\rangle + \beta\,|-\rangle$, ancillas are both in $|1\rangle$.
- Encoding: mapping to $\alpha\,|+++\rangle + \beta\,|---\rangle$.
- Phase flip changes $|\pm\rangle$ to $|\mp\rangle$.
- Decoding and correction: majority vote.
- Resetting the ancillas, while preserving the information of system qubit.

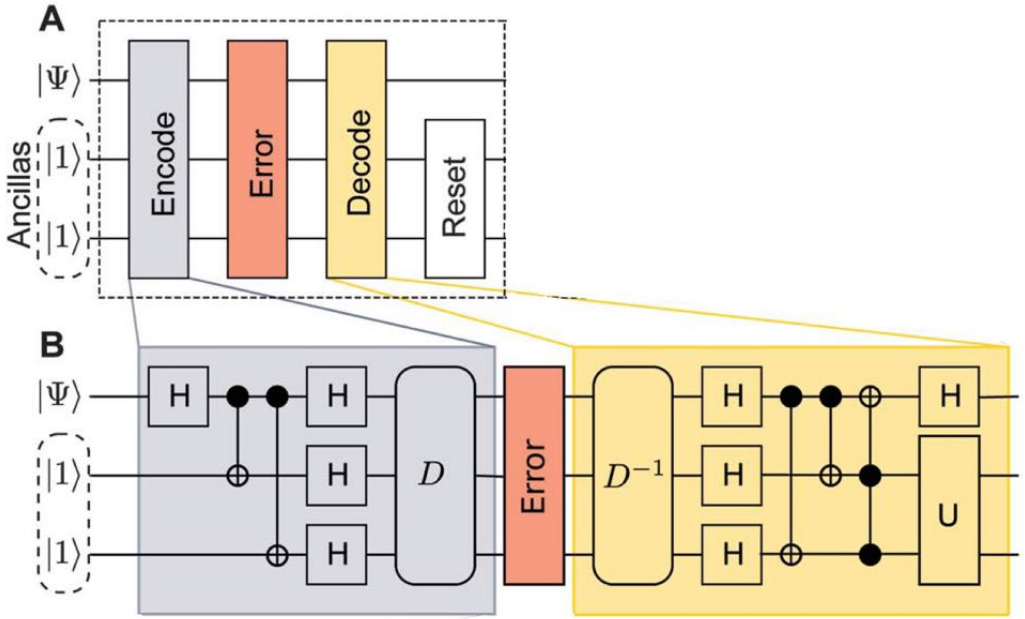

Figure: Quantum circuit for QEC - textbook implementation.

4 CNOT gates and 1 Toffoli gates $\longrightarrow$ fidelities CNOT(92%) Toffoli (80%).

Major improvement with global Mølmer–Sørensen entangling operations (99%).
Optimization toolbox:

1. high-fidelity quantum operations,
2. optimized pulse sequence,
3. qubit-reset technique with negligible effect on the system of qubits.

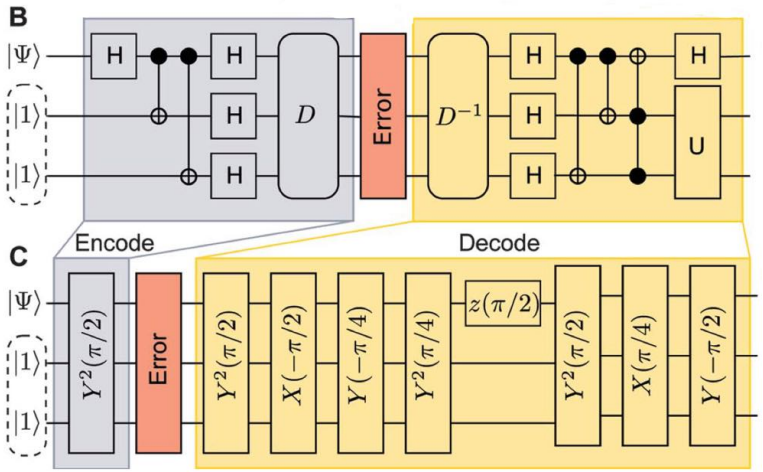

Figure: Optimized pulse sequence for a single error-correction cycle.

- D commutes with any phase errors:
  $D\,(\mathrm{Error})\,D^{-1} = (\mathrm{Error})\,DD^{-1} = (\mathrm{Error})$.
- U increases the space of optimized solutions.

Quantum Computation with Ions in Thermal Motion

Anders Sørensen and Klaus Mølmer
Institute of Physics and Astronomy, University of Aarhus, DK-8000 Århus C, Denmark
(Received 26 June 1998; revised manuscript received 25 November 1998)

We propose an implementation of quantum logic gates via virtual vibrational excitations in an ion-trap quantum computer. Transition paths involving unpopulated vibrational states interfere destructively to eliminate the dependence of rates and revolution frequencies on vibrational quantum numbers. As a consequence, quantum computation becomes feasible with ions whose vibrations are strongly coupled to a thermal reservoir. [S0031-9007(99)08589-0]

- Method to construct states: $|\psi\rangle = \frac{1}{\sqrt{2}}\left[e^{i\phi_g}|gg\cdots g\rangle + e^{i\phi_e}|ee\cdots e\rangle\right]$.
- Address each ion through single laser, quantum logic gates through off-resonant laser pulses.
- Use it together with ancillas to perform encoding procedure.
- Independent of quantum vibrations and temperature.

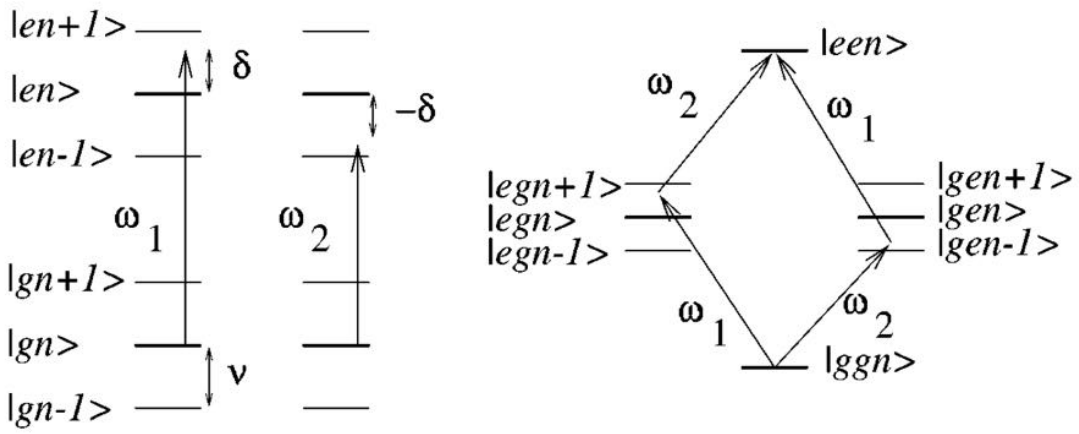

Figure: Energy levels and laser detunings.

Interaction Hamiltonian: $H_{int} = \frac{\hbar\Omega}{2}\mathbf{E}\cdot\mathbf{S} = \sum_i \frac{\hbar\Omega_i}{2}\left(\sigma_{+i}e^{i\left[\eta_i\left(a+a^\dagger\right)-\omega_i t\right]} + h.c.\right)$.

Lamb-Dicke parameter: $\eta = 2\pi z_0/\lambda, \quad z_0 = \sqrt{\hbar/2NM\nu}$.

Rabi frequency between $|ggn\rangle$ and $|een\rangle$ in the second order perturbation theory:

$$\left(\frac{\bar{\Omega}}{2}\right)^2 = \frac{1}{\hbar^2}\left|\sum_m \frac{\langle een|\, H_{int}\, |m\rangle \langle m|\, H_{int}\, |ggn\rangle}{E_{ggn} + \hbar\omega_i - E_m}\right|^2 \quad \Rightarrow \quad \bar{\Omega} = \frac{(\Omega\eta)^2}{2\,(\nu-\delta)}.$$

$\eta_1 = \eta_2 = \eta$ and $\Omega_1 = \Omega_2 = \Omega$, $\delta = \omega_1 - \omega_{eg}$.

When summed over all ions, the couplings lead to the spin Hamiltonian:

$$H = 4\frac{\chi}{\hbar}J_x^2, \quad \chi = \frac{\eta^2\Omega^2\nu}{2\left(\nu^2-\delta^2\right)}.$$

Time evolution operator: $U(t) = \exp\left(-i4\frac{\chi}{\hbar^2}J_x^2 t\right) \longrightarrow$ population becomes distributed on all states.

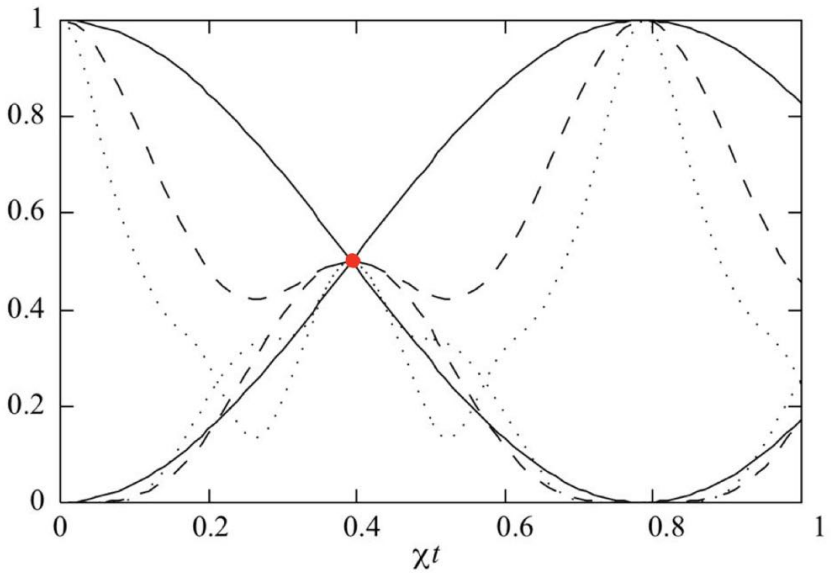

Figure: Time evolution of the population of the joint ground state, and the joint excited state. Different curves correspond to different number of ions.

At time $t = \pi/8\chi$ populations equal one half $\longrightarrow$ maximally entangled states of high fidelity.

In our experiment: three $^{40}Ca^{+}$ ions, each qubit in the $|1\rangle = 4S_{1/2}(m_J = -1/2)$ and $|0\rangle = 3D_{5/2}(m_J = -1/2)$ states.
Universal set of gates:

- Collective local operations: $X(\theta) = \exp\left(-iS_x\theta/2\right)$ and $Y(\theta) = \exp\left(-iS_Y\theta/2\right)$.
- Single-qubit operations: $Z_k(\theta) = \exp\left(-i\sigma_z^{(k)}\theta/2\right)$.
- Collective entangling Molmer-Sorensen operations: $Y^2(\theta) = \exp\left(-iS_y^2\theta/2\right)$, with $S_{x,y} = \sum_{k=1}^{3} \sigma_{x,y}^{(k)}$.

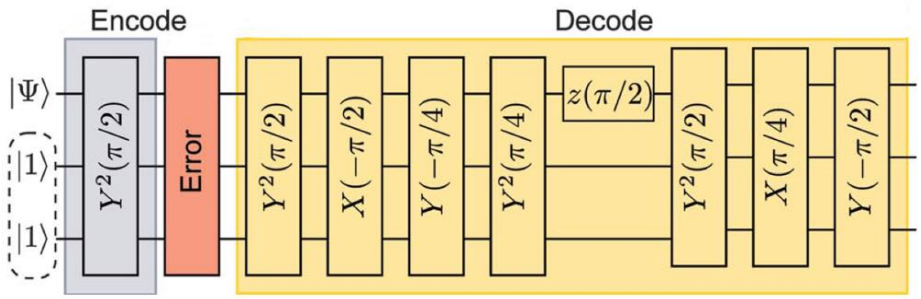

Experimental cycle: **1.** cooling of ions to the motional ground state, **2.** applying the manipulating laser pulses, **3.** measuring the population of the qubit states.
Procedure repeated 1000 times.

Reset of ancillas

1. Ancilla qubits in $|0\rangle$ transferred into $|S'\rangle = 4S_{1/2}(m_J = 1/2)$.
2. Population in $|S'\rangle$ excited to the $4P_{1/2}(m_J = -1/2)$ by a laser beam at 397nm.
3. Population from the $4P_{1/2}$ spontaneously decays to the $4S_{1/2}$.

* population loss into $3D_{3/2}$ avoided by repump laser resonant with $3D_{3/2} - 4P_{1/2}$ transition.

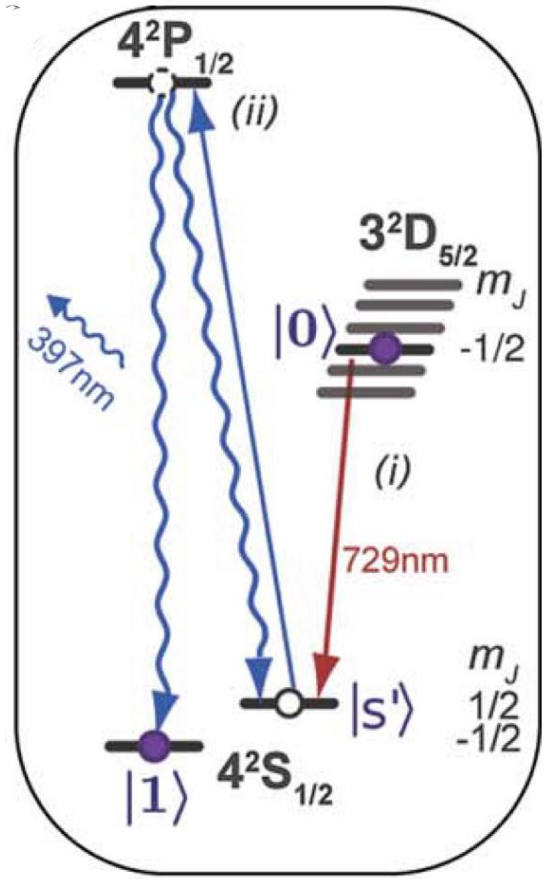

Figure: Schematic of the reset procedure.

Operational quality of the QEC protocol

Expose it to correctable errors $\rightarrow$ single-qubit phase-flips.
Ideally, encoded qubit experiences identity operation.
Experimentally, process characterized by quantum process tomography $\rightarrow$ process matrix χ.
Process fidelity: $F_{proc} = Tr\,(\chi \cdot \chi_{id})$.

Number of QEC cycles	No error F_{none}	Optimized no error F_{opt}	Single-qubit errors F_{single}	Optimized single-qubit errors F_{sopt}
0	97(2)	97(2)	–	–
1	87.5(2)	90.1(2)	89.1(2)	90.1(2)
2	77.7(4)	79.8(4)	76.3(2)	80.1(2)
3	68.3(5)	72.9(5)	68.3(3)	70.2(3)

Process fidelity for a single uncorrected qubit as well as for one, two, and three error-correction cycles. F_{none} is the process fidelity without inducing any errors. F_{single} is obtained by averaging over all single-qubit errors. F_{opt} and F_{sopt} are the respective process fidelities where constant operations are neglected.

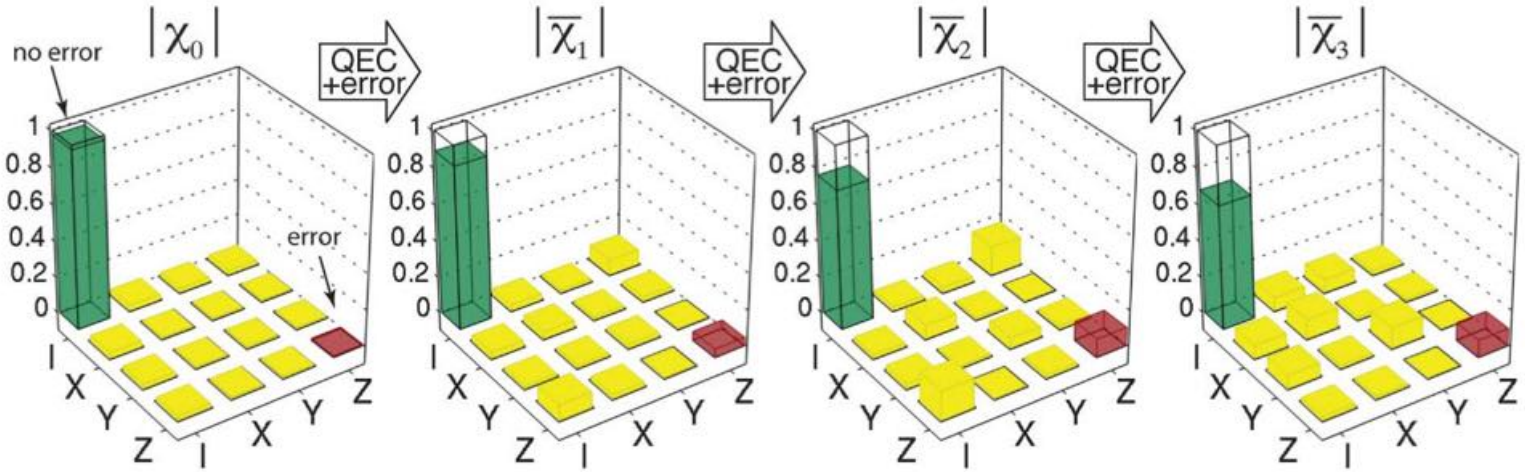

Figure: Mean single-qubit process matrices $\bar{\chi}_n$ (absolute value) for n QEC cycles with single-qubit errors. Transparent bars show the identity process matrix, and the red bar denotes a phase-flip error. Process matrices were reconstructed from a data set averaged over all measured expectation values.

Behavior of the QEC algorithm in the presence of two most prominent noise types:

- Uncorrelated: short laser pulse on the detection transition after encoding.
- Correlated: fluctuations in the magnetic field strength and the laser frequency.

Presence of noise type verified by the probability of simultaneous n-qubit flips.

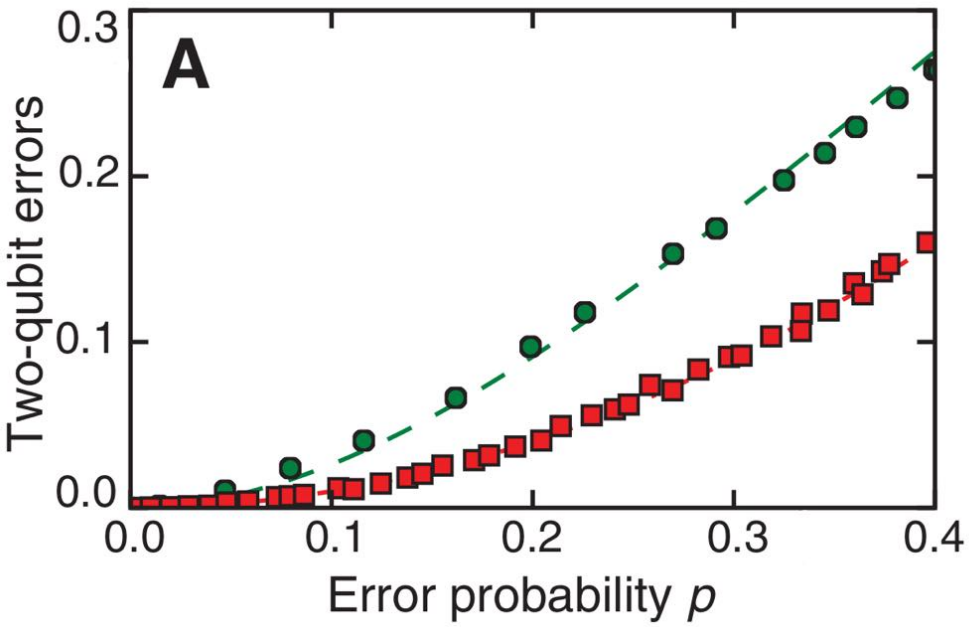

Figure: Probability of simultaneous two-qubit phase flips as a function of the single-qubit phase flip probabilities for uncorrelated (square) and correlated (circle) noise measured by a Ramsey-type experiment.

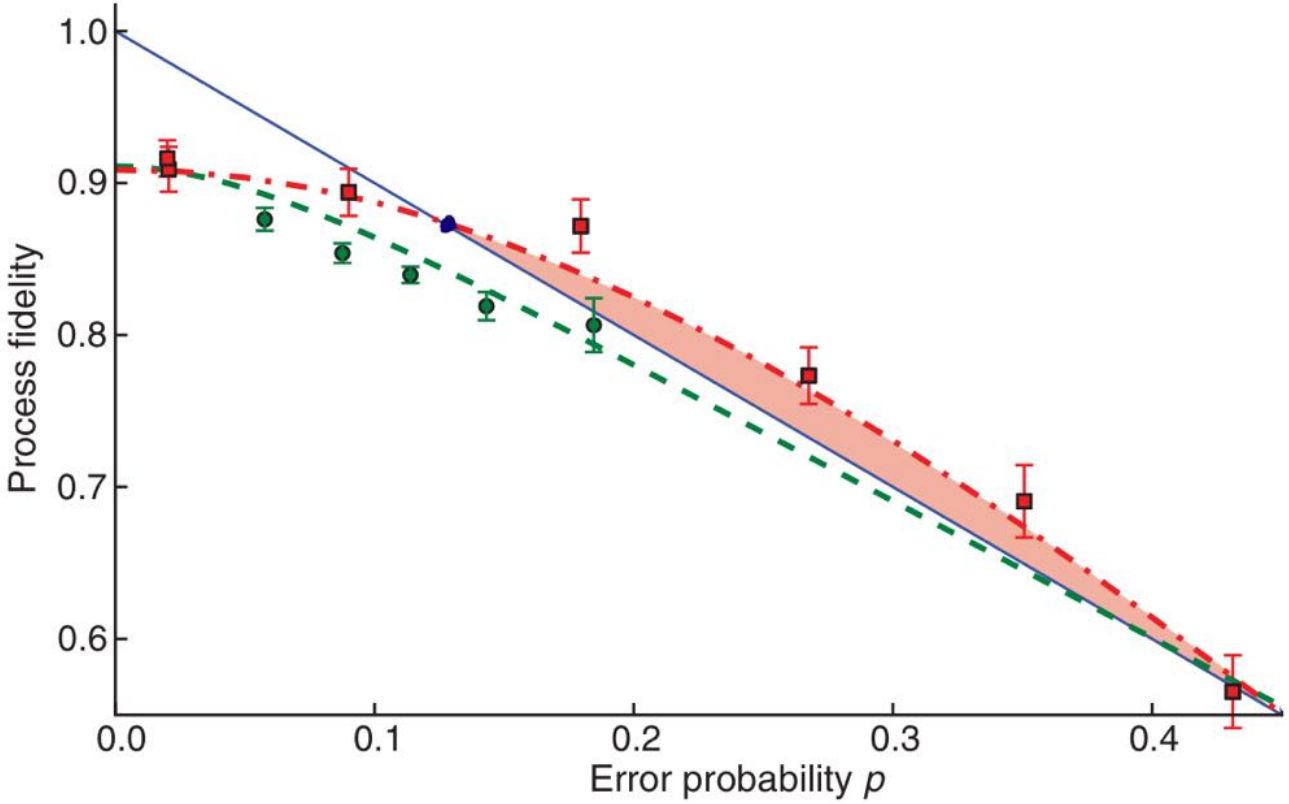

Figure: Process fidelity of the QEC algorithm in the presence of correlated (circle) and uncorrelated (square) phase noise as a function of the single-qubit phase flip probability. The theory is shown for an unencoded qubit (solid line), a corrected qubit in presence of correlated (dashed line), and uncorrelated noise (dash-dot line).

Summary and outlook

- Implementation of a repeatable QEC algorithm with 3 trapped ions.
- Used global-entangling and local-qubit operations in an optimized pulse sequence.
- For uncorrelated errors, a corrected qubit performs better than an uncorrected qubit for a range of probabilities.
- Algorithm extended to 5 qubits.[1]
- Work in other models:
  - *"Realization of Three-Qubit Quantum Error Correction with Superconducting Circuits", Reed, M. D.; DiCarlo, L.; Nigg, S. E.; Sun, L.; Frunzio, L.; Girvin, S. M.; Schoelkopf, R. J. (2012).*
  - *"Quantum optical coherence can survive photon losses using a continuous-variable quantum erasure-correcting code", Lassen, M.; Sabuncu, M.; Huck, A.; Niset, J.; Leuchs, G.; Cerf, N. J.; Andersen, U. L. (2010).*

[1] Optimal control of entangling operations for trapped-ion quantum computing, V. Nebendahl, H. Häffner, and C. F. Roos, Phys. Rev. A 79, 012312